International Journal of Thermal Sciences 49 (2010) 741–748

Contents lists available at ScienceDirect

International Journal of Thermal Sciences

journal homepage: www.elsevier.com/locate/ijts

Study on onset of nucleate boiling in bilaterally heated narrow annuli

Y.W. Wu, G.H. Su*, B.X. Hu, S.Z. Qiu

State Key laboratory of Multiphase Flow in Power Engineering, Department of Nuclear Science and Technology, Xi'an Jiaotong University, Xi'an city 710049, China

ARTICLE INFO

Article history:
Received 2 March 2009
Received in revised form
12 November 2009
Accepted 24 November 2009
Available online 31 December 2009

Keywords:
Narrow annular channel
ONB
Bilateral heating

ABSTRACT

Onset of nucleate boiling (ONB) experiments using deionized water as working fluid have been conducted in a range of pressure from 1 to 4 MPa, mass flow velocity from 56 to 145 kg/m^2 s and wall heat flux from 9 to 58 kW/m^2 for vertical narrow annuli with annular gap sizes of 0.95, 1.5 and 2 mm. We found that the ONB sometimes occurs only on outer annulus surface, sometimes occurs only on inner annulus surface and sometimes occurs on both annulus surfaces. The heat flux of the other side has great influence on the heat flux of the ONB and the latter will decrease with the increase of the heat flux of the other side. It is also found that the heat flux of the ONB increases with the increase of the pressure, the mass flux and wall superheat. However, the heat flux of the ONB will decrease as the gap size increases in narrow annuli. The heat flux of the ONB in narrow annuli is much lower than that calculated by correlations for conventional channels and a new correlation, which has good agreement with the experimental data, has been developed for predicting the heat flux of the ONB in narrow annuli.

1. Introduction

Heat transfer enhancement technology in narrow channels has attracted more and more attentions because of such advantages as flexibility design, high heat transfer efficiency, low heat transfer temperature difference and compacted structure without complex surface treatment. Now narrow channels have been widely used in many industrial areas, such as refrigeration, spaceflight, microelectronics, reactor engineering and thermal engineering. Double tube heat exchanger which uses the narrow annular channel as its key component is one of the most advanced compact exchangers at present. The narrow annular channel uses dual-tube structure for heat exchange and the gap size between the two tubes is very small, only 0.5–2.5 mm. Compared to the conventional circular tube, the narrow annular channel's heat exchange area is nearly two times per unit volume, and also the narrow channel itself could enhance heat transfer [1–3], thus double tube heat exchangers have very high heat transfer capacity and research on heat transfer characteristics in narrow annuli has great industrial significance.

It is known that bubbles will begin to generate at certain heat flux when fluid flows through heated channels, and this is the onset of nucleate boiling (ONB). After the ONB, flow pattern becomes two-phase from single phase, and mechanisms for flow and heat transfer change. Obviously, the study on ONB is very important. Thus carrying out study on ONB in narrow annuli is significant.

So far, many researchers have carried out research on the ONB in narrow channels. Ghiaasiaan and Chedester [4] experimentally studied incipient flow boiling characteristics in micro-tubes with diameters in the 0.1–1 mm range. They found that the heat flux of the ONB in the experiment was higher than that calculated using correlations for conventional channels. They also pointed out that in micro-tubes the main factor affecting ONB was the thermal capillary force acting on bubbles. Hapke et al. [5] investigated ONB in a vertical evaporator pipe with an internal diameter of 1.5 mm. They found that the wall surface superheat in narrow channels is higher than conventional channels when the ONB occurs and the wall superheat will become lower with higher mass flux when the heat flux keeps invariant. Qi et al. [6] conducted an experimental study concerning the flow boiling of liquid nitrogen in the micro-tubes with the diameters of 0.531, 0.834, 1.042 and 1.931 mm. It is found that the mass flux drops suddenly while the pressure drop increases at ONB, and apparent wall temperature hysteresis in the range of 1.0–5.0 K occurs. They modified Thom's model [7] to predict the wall superheat and heat flux at ONB which kept consistent with the experimental data. Qu and Mudawar [8] performed experiments to measure the incipient boiling heat flux in a heat sink containing twenty-one rectangular (231 μm wide and 713 μm deep) micro-channels using deionized water as working fluid. They found that most bubbles distributed at the bottom of the channels and bubbles didn't rupture immediately as they do in large channels but departed into the liquid flow. They proposed

* Corresponding author. Tel./fax: +86 29 82663401.
E-mail address: ghsu@mail.xjtu.edu.cn (G.H. Su).

1290-0729/$ – see front matter © 2009 Elsevier Masson SAS. All rights reserved.
doi:10.1016/j.ijthermalsci.2009.11.010

Nomenclature

A	heat transfer area, $A = \pi dL$, m^2
A_f	flow area of the test section, m^2
C_p	specific heat capacity, kJ/kg K
d	tube diameter, m
d_h	heated equivalent diameter, $d_h = d_{oi} - d_{io}$, m
G	Mass flux, kg/m^2 s
h_{fg}	latent heat of vaporization, kJ/kg
I	electric current, A
k	water thermal conductivity, W/m K
L	heated length, m
L_z	length from the calculated water temperature point to the inlet of the test section, m
p	system pressure, MPa
q	heat flux, kW/m^2
Re	Reynolds number
r^*_{max}	maximum cavity radius, m
s	gap size, mm
t	temperature, K
U	electrode voltage, V
υ_{fg}	liquid-gas specific volume difference at saturated pressure, $\upsilon_{fg} = \upsilon_g - \upsilon_f$, m^3/kg

Greek symbols

φ	contact angle, rad
σ	surface tension, N/m
Δt_{sat}	wall superheat, $\Delta t_{sat} = t_w - t_s$, K
$\Delta\rho$	difference between the saturated liquid density and saturated vapor density, $\Delta\rho = \rho_f - \rho_g$, kg/$m^3$
ρ_f	saturated liquid density, kg/m^3
ρ_g	saturated vapor density, kg/m^3
η	thermal efficiency
μ	coefficient of kinetic viscosity, kg/m s

Subscripts

av	average
f	fluid
i	inside tube
ii	inner surface of inside tube
in	inlet
io	outer surface of inside tube
o	outside tube
oi	inner surface of outside tube
oo	outer surface of outside tube
w	wall
s	saturated

a comprehensive model to predict the incipient boiling heat flux, accounting for the complexities of bubble formation along the flat and corner regions of a rectangular flow channel, as well as the likelihood of bubbles growing sufficiently large to engulf the entire flow area of a micro-channel. Chen et al. [9] investigated subcooled boiling incipience on a highly smooth micro-scale heater submerged in FC-72 liquid. They observed that bubble incipience on the micro-heater was an explosive process, just as gas-liquid phase transition. With the explosive process, wall bubbles could generate with low wall superheat. Kamil et al. [10] found that the minimum heat flux when ONB occurred is related with the thermophysical properties of the working fluid. Based on this, they founded models and obtained a unified correlation for nine different fluids, together covering wide ranges of heat flux, submergence and inlet liquid subcooling. Su et al. [11] studied incipient boiling of water in narrow annuli with the equivalent diameters of 2 mm and 3 mm. They found that the heat flux of the ONB was independent of system pressure, increased with increasing mass flux and decreased with decreasing gap size. Also they developed a correlation to predict the heat flux of the ONB and the relative error was below 15%.

As described above, flow boiling heat transfer in micro-tubes or rectangular micro-channels has been investigated extensively. However, no enough attentions have been paid to the onset of nucleate boiling in narrow annuli and no uniform cognition has been formed on the heat transfer mechanisms. This study was aimed to analyze the factors affecting ONB in narrow annuli and to predict the heat flux of the ONB.

2. Experiment

2.1. Experimental loop

The experimental test loop is shown schematically in Fig. 1. It consisted of two main loops, namely, the primary and the secondary loops. The secondary loop, which was connected to the primary one through the condenser, was used to condense the fluid in the primary loop. The primary loop contained a circulating water pump, a pressurizer, a nitrogen cylinder, a feedwater tank, a u-type preheater, a serpentine preheater, two mass flow meters, a test section, a condenser, a measuring and monitoring system, valves and connecting pipes. The secondary loop contained a water tower, a condenser, a pump, a water tank and a water tower. All parts were made up of SUS304 stainless steel as far as possible, to minimize the corrosion and to allow easy cleaning. And use of flanged joints was maximized for easy maintenance between experiments.

The temperature and mass flow rate in the secondary loop must be controlled to have enough cooling capacity to condense the fluid in the primary loop and subcool it to a much lower temperature than the saturated temperature. Two power supplies were used to heat the inside and outside tubes in the test section respectively. The fluid circulated by the pump in the primary loop flowed through the preheaters, the flow meters, and then it was fed into the test section and flowed into the condenser. The mass flux of the test section can be regulated by adjusting the gate opening of the

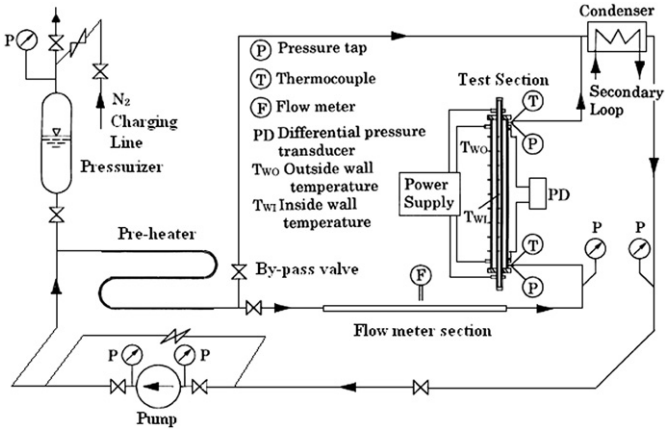

Fig. 1. Schematic diagram of the experimental apparatus.

bypass valve. The system pressure can be regulated by adjusting charge of nitrogen through the nitrogen charging line. The mass flow rate and system pressure should be further adjusted by the needle valve at the upstream of the flow meter section and the power of the heater in the pressurizer respectively, in order to control them at required level more precisely.

2.2. Test section

Three test sections were used in this study. As shown in Fig. 2, they were composed of two concentric cold-drawn SUS304 stainless steel tubes, with the fluid flowing through the annular space between the two tubes. The measured roughnesses of the inside and outside tubes have an order of magnitude of 5 μm. The test sections had the following geometrical parameters: 700 mm in length, 10 mm i.d. and 2 mm thickness of outside tube, 8.1 mm, 7 mm and 6 mm o.d. and 1 mm thickness of inside tube. Thus the corresponding annular gap sizes of the three test sections were 0.95 mm, 1.5 mm and 2 mm respectively. The inside and outside tubes of the test section were heated by two low voltage and high current DC power supplies respectively and thus the heat fluxes of inside and outside tubes can be regulated separately. NiCr–NiSi thermocouples with Φ0.5 mm were spot-welded on the outer surface of fifteen cross-sections at each interval of 25 mm along axial direction of the outside tube. In each horizontal cross section, four thermocouples were arranged on the outside tube with 90° apart and the average value of them was regarded as the outer wall surface temperature of the outside tube in this section. Because thermocouples could not be spot-welded directly on the surface of inside tube, the following method of temperature measurement was employed. Firstly, fifteen NiCr–NiSi armoured thermocouples with Φ0.5 mm were arranged on the work table according to the thermocouple distribution of the outside tube and bundled up one by one. Then the thermocouples were wrapped using a thin flexible electrical insulation mica belt to keep electrical insulation between the thermocouples and the inside tube, and a thin, long thermocouple assembly came into being. Finally, the thermocouple assembly was inserted into the inside tube carefully to make the locations of the

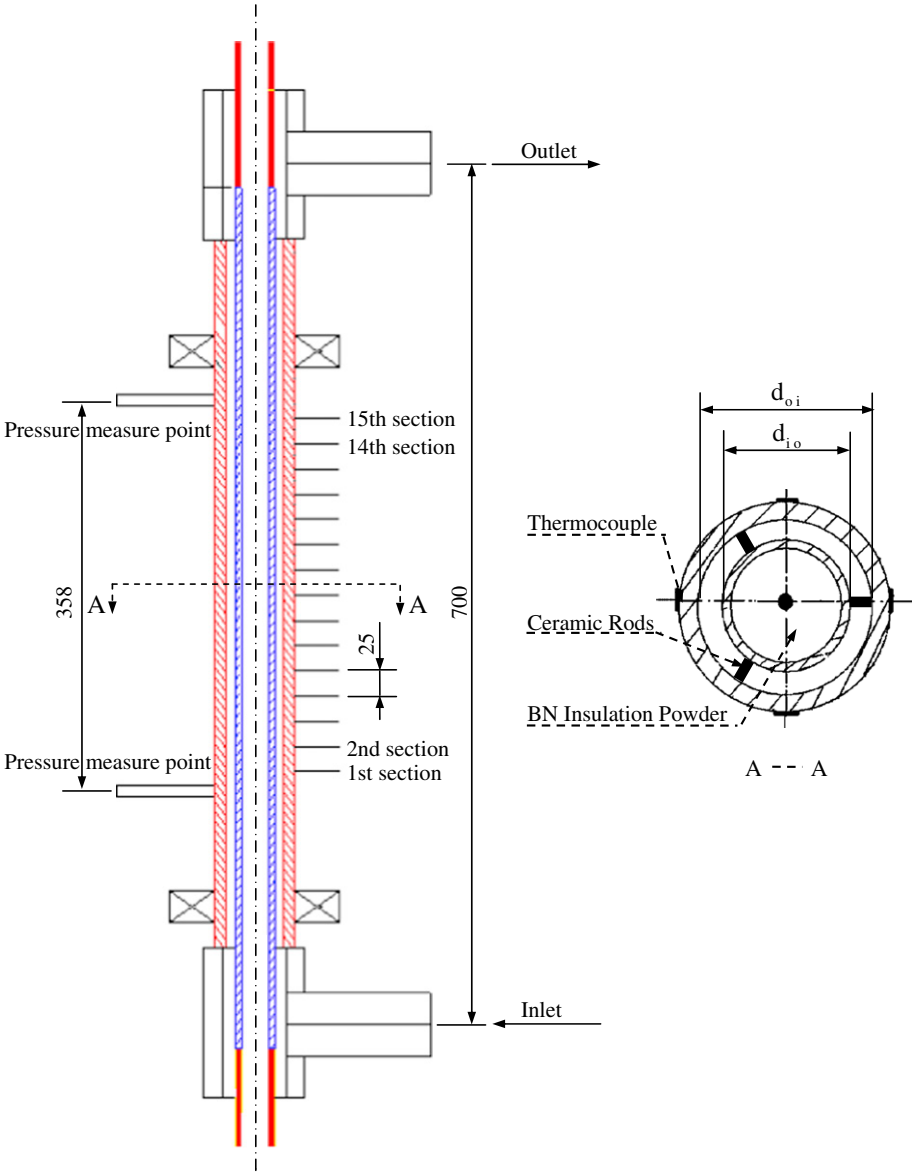

Fig. 2. Schematic diagram of the test section.

thermocouples be in one-to-one correspondence with that of the thermocouples on the outside tube. The space between the inside tube and the thermocouple assembly was filled with BN powder to improve electrical insulation and thermal conduction. Under steady experimental conditions, it was concluded that the inside space of the inside tube was thermal insulation according to the heat transfer conditions and the temperature distribution along the inside vertical space was just the inner wall surface temperature distribution along the inside tube.

It was very important to ensure the concentricity and the electrical insulation between the inside and outside tubes. Therefore, the composing tubes were made of specially processed straight stainless steel tubes with linearity error less than 0.01% and three small ceramic rods were arranged at the same cross section with equal angular interval at the middle of test section as shown in Fig. 3.

To thermally insulate the test section from the environment, the whole test section is firstly covered by silicon-aluminium glass fiber with 120 mm in thickness, a wire heater with 3 kW in maximum power winded the outside of this heat insulator to compensate heat loss of the test section, and then another silicon-aluminium glass fiber with 50 mm in thickness wraps the whole test section. Two thermocouples are located in the different places of the inner silicon-aluminium glass fiber along radial direction. By controlling the power of the wire heater and making the measured values by the two thermocouples equal to each other as possible, then good heat insulation could be acquired for the test section.

2.3. Instrumentation

The wall temperatures of test sections are detected by NiCr–NiSi thermocouples and analyzed by an IMP (Isolated Measurement Pod) distributed data acquisition system which could be used in continuous real-time data acquisition of slowly changing analog signals (e.g. voltage, electric current, electric resistance, temperature, pressure, mass flux) and could be used in input and output controls of various types of digital signals and output control of analog quantity in various industrial processes and other bad conditions.

Fluid temperatures at the pump inlet, condenser inlet and outlet, preheater inlet and outlet, and test section inlet and outlet are measured by NiCr–NiSi armoured thermocouples of Φ1.0 mm. The flow rate into the test section is measured by a venturi flow meter. The pressure is measured by using piezo capacitive type transducer.

2.4. Test conduct

Experiments have been performed for upward flow of deionized water with changing pressure, mass flux and wall heat flux under single-sided heating and two-sided heating conditions. Ranges of parameters tested in the experiment are summarized in Table 1.

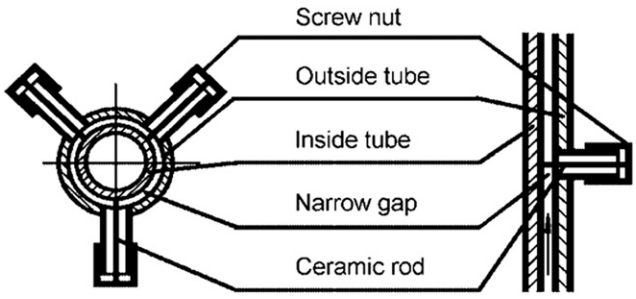

Fig. 3. Schematic description of the holding concentricity.

The water in the loop is circulated and boiled for about half an hour prior to the experiment to reduce the possible non-condensable gas content. Then the water is cooled to a designated temperature so that the desired inlet temperature could be easily obtained and the valves are set to obtain the desired flow rate. During the experiments, the pressure of the test loop is regulated by adjusting the regulator of nitrogen cylinder bottle.

3. Data reduction

The heat fluxes for the inside tube, outside tube and the average tube could be obtained by the following formulas:

$$q_i = \frac{Q_i}{A_i}, \quad Q_i = \eta \cdot U_i \cdot I_i \tag{1}$$

$$q_o = \frac{Q_o}{A_o}, \quad Q_o = \eta \cdot U_o \cdot I_o \tag{2}$$

$$q_{av} = \frac{Q_o + Q_i}{A_o + A_i} = \frac{q_o A_o + q_i A_i}{A_o + A_i} = \frac{A_o}{A_o + A_i} q_o + \frac{A_i}{A_o + A_i} q_i \tag{3}$$

where η is the thermal efficiency and could be obtained by thermal balance experiment.

As mentioned in Section 2.2, the outer surface temperatures of outside tube are measured by Φ0.5 mm thermocouples spot-welded on the outer surface and the inner surface temperatures of inside tube are measured by thermocouples assembly inserted into the inside tube. Therefore, the outer surface temperatures of outside tube t_{woo} and the inner surface temperatures of inside tube t_{wii} can be directly measured using thermocouples. However, for experimental data reduction, we need the inner surface temperatures of outside tube t_{woi} and the outer surface temperatures of inside tube t_{wio}. Thus, for this purpose, a progress of conduction in a column with average heat sources is evaluated and the final results can be written as

$$t_{woi} = t_{woo} - \left(\frac{q_o}{k_w}\right)\left(\frac{d_{oi}}{d_{oo}^2 - d_{oi}^2}\right)\left(\frac{d_{oo}}{2}\right)^2 \times \left[2\ln\left(\frac{d_{oo}}{d_{oi}}\right) + \left(\frac{d_{oi}}{d_{oo}}\right)^2 - 1\right] \tag{4}$$

$$t_{wio} = t_{wii} - \left(\frac{q_i}{k_w}\right)\left(\frac{d_{io}}{d_{io}^2 - d_{ii}^2}\right)\left(\frac{d_{ii}}{2}\right)^2 \times \left[\left(\frac{d_{io}}{d_{ii}}\right)^2 - 2\ln\left(\frac{d_{io}}{d_{ii}}\right) - 1\right] \tag{5}$$

The water temperature t_f could be calculated by the imposed power from inside and outside tubes, and the inlet temperature of the water by the following equation:

$$t_f = t_{f,in} + (\pi \cdot d_{io} \cdot q_i + \pi \cdot d_{oi} \cdot q_o) \cdot L_z / (G \cdot A_f \cdot C_p) \tag{6}$$

In this study, all the measuring devices were calibrated by the authoritative institutes. Uncertainties of the mass flux, the system

Table 1
Experimental conditions.

Parameters	Range
Pressure, p (MPa)	0.93–3.85
Mass flux, G (kg/m^2 s)	56.15–144.99
Gap size, s (mm)	0.95, 1.5, 2
Reynolds number, Re	1319.67–3871.81
Heat flux of outside tube, q_o (kW/m^2)	12.96–43.15
Heat flux of inside tube, q_i (kW/m^2)	9.71–57.05

pressure, the measured heat fluxes of the two heated surfaces etc. are estimated according to the procedures proposed by Kline and McClintock [12] for the propagation of errors in physical measurement. The results from this uncertainty analysis are summarized in Table 2.

4. Results and discussion

4.1. Determination of ONB

According to the mechanisms of flowing heat transfer, for single phase convection the wall surface temperature increases linearly along the heating length of the channel on the condition of constant heat flux. Only when the temperature of the liquid near the wall exceeds the saturation temperature and reaches certain superheat, bubbles could generate. The wall surface temperature will keep almost constant after the occurrence of ONB. Thus, the occurrence of ONB can be judged by observing the wall temperature along the heated length of the channel [13].

As shown in Fig. 4, the first point of the wall temperature deviating from linear increase is regard as the ONB and the wall temperature basically maintaines at a constant after the ONB. Also, the ONB point was verified by the flow boiling curve [6]. There is little difference between the two results by the different judging methods. It should be mentioned that the ONB sometimes occurs only on outer annulus surface, sometimes occurs only on inner annulus surface and sometimes occurs on both annulus surfaces for the fluid in the narrow annular channel was heated by DC current power on each side of the annular channel.

4.2. Analysis of parametric trends

The factors affecting the heat flux of ONB may be the system pressure, the mass flux, the wall superheat, the gap size and so on. The effects of the pressure, the mass flux and the local wall superheat on the heat flux of the ONB are the same as they do in conventional channels. The heat flux of the ONB in narrow annuli will increase with the increase of pressure, mass flux and the local wall superheat. Here, we analyzed the effects of the gap size and the heat flux of the other side on the heat flux of the ONB in detail.

Fig. 5 shows that at given system pressure, mass flux, and heat flux of the inner tube, the q_{ONB} will decrease as s increases in narrow annuli. When s is small, boiling incipience in narrow annuli may be controlled by the thermocapillary force that tends to suppress the microbubbles that form on wall cavities. Therefore, the heat flux of $s = 0.95$ mm is larger than that of $s = 2$ mm. When s is very large, the narrow annuli will become conventional channels.

Table 2
Summary of the uncertainty analysis.

Parameters	Uncertainty
Annular channel geometry	
Length and diameter, L and d (m)	±0.25%
Area, A (m^2)	±0.5%
Parameter measurement	
Wall temperature, t_w (K)	±0.75%
Inlet water temperature, $t_{f,in}$ (K)	±0.75%
System pressure, p (MPa)	±0.25%
Mass flux, G (kg/m^2 s)	±0.25%
Voltage, U (V)	±0.5%
Current, I (A)	±0.1%
Data acquisition system	±0.02%
Parameter derived	
Imposed heat flux, q (kW/m^2)	±3%
Water temperature, t_f (K)	±1.81%

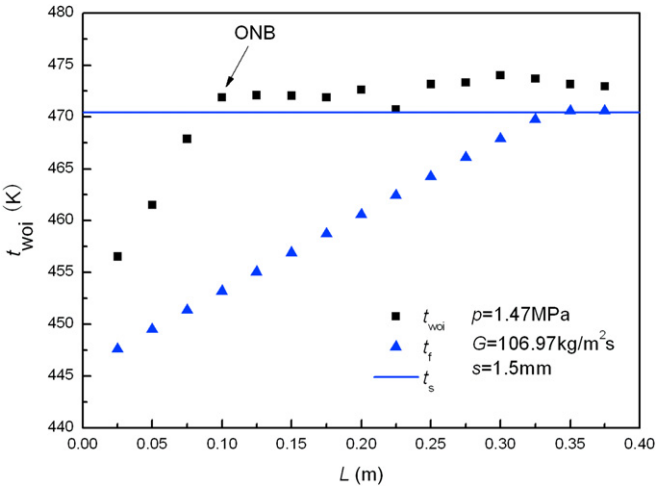

Fig. 4. Determination of the ONB.

The q_{ONB} in a conventional channel is higher than that in the narrow annular channel as described in the following section. Therefore, there must be a critical size for the gap size where the required heat flux of the ONB is the lowest under the same conditions. However, the critical size could not be given based on the present experiments, but it is sure to exist and greater than 2 mm.

The fluid was heated by DC current power on each side of the annular channel. The different heat fluxes on each surface contribute much to the location of ONB and the corresponding heat flux. The heat flux of the ONB will decrease with the increase of the heat flux on the other tube as shown in Fig. 6. On the same inlet conditions, the fluid in narrow annuli will absorb more heat from the other tube when the other tube heat flux is large. Bubbles will generate on the wall surface more easily and hereby the corresponding heat flux is small.

4.3. Compared to existed correlations

For conventional channels, many researchers have carried out research on ONB and developed many correlations for conventional

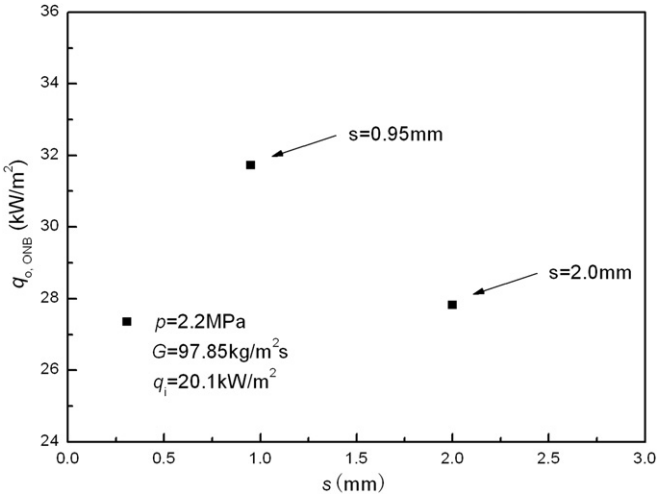

Fig. 5. Effect of the gap size on the heat flux of the ONB.

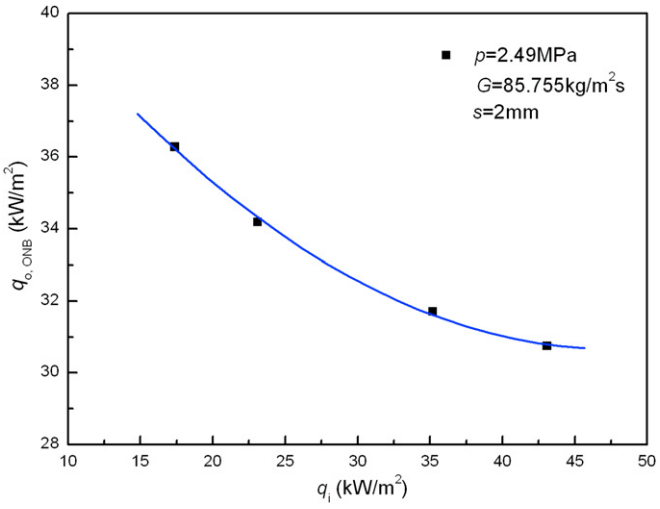

Fig. 6. Effect of the other side heat flux on the heat flux of the ONB.

channels. The method of Bergles and Rohsenow [14] was most widely used, and they proposed the following equation for the incipient boiling condition in the case of the surface cavities of all sizes are available for nucleation:

$$q_{\mathrm{ONB}} = 15.516 \cdot p^{1.156}[1.8(t_{\mathrm{w}} - t_{\mathrm{s}})]^{\frac{2.047}{p^{0.0234}}} \tag{7}$$

Davis and Anderson [15] extended this analysis and introduced the contact angle as a variable for the ONB condition. Their analysis gave the heat flux condition at ONB as

$$q_{\mathrm{ONB}} = \frac{k_{\mathrm{f}} h_{\mathrm{fg}}}{C(8\sigma t_{\mathrm{s}} \upsilon_{\mathrm{fg}})}(t_{\mathrm{w}} - t_{\mathrm{s}})^2 \tag{8}$$

where $C_1 = 1 + \cos\varphi$ and here $\varphi = \pi/2$ for hemispherical bubbles.

Hino and Ueda [16] performed ONB experiments using R-113 as working fluid in an annulus with a uniformly heated inner tube. In the case where the upper limit of available cavity sizes is restricted to radius $r^*_{\max}$, the incipient boiling condition is expressed as follows:

$$q_{\mathrm{ONB}} = \frac{k_{\mathrm{f}}}{r^*_{\max}}(t_{\mathrm{w}} - t_{\mathrm{s}}) \times 10^{-3} - \frac{2\sigma k_{\mathrm{f}} t_{\mathrm{s}}}{h_{\mathrm{fg}} \rho_{\mathrm{g}} (r^*_{\max})^2} \times 10^{-6} \tag{9}$$

Fig. 7 shows the relation between the heat flux and the wall superheat at the position of incipient boiling obtained from the experimental data and the above three correlations. As shown in Fig. 7, it is found that the calculated heat flux using the two correlations for conventional channels is much higher than the experimental heat flux in narrow annuli. Also, the heat flux of the ONB, especially with high wall superheat, calculated by Eqs. (7) and (8) for conventional channels is higher than that calculated by Eq. (9) for narrow annuli with $r^*_{\max} = 5$ μm. It is shown that the correlations for conventional channels cannot be used in narrow annuli. Also, it is worth noting that the heat flux of ONB in the narrow annular channel is far less than that in micro-tubes and the latter is even higher than that in conventional channels [4]. The results show that the occurrence mechanism of the ONB is different from that in conventional channels or micro-tubes. The reasons may be as follows: On the one hand, the structure of the annular channel, which uses dual-tube structure for heat exchange, is different from that of conventional channels or micro-tubes. In subcooled boiling, the velocity and temperature gradients near the

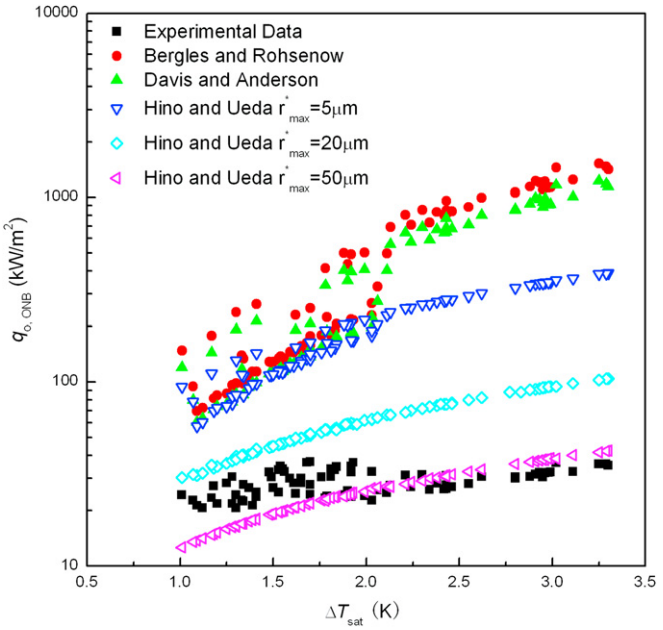

Fig. 7. Comparison of the calculated data with the experimental data.

walls of narrow annuli can be different from that of conventional channels or micro-tubes, rendering forces such as thermocapillary force and the lift force resulting from the liquid velocity gradient are significant, and the sizes of the released bubbles may be different from those in conventional channels or micro-tubes [17]. The occurrence of bubbles significantly impacts the onset of nucleate boiling [18]. Therefore, the heat flux of ONB in the narrow annular channel is different from that in conventional channels or micro-tubes. By the way, the detail situations of the released bubbles from the walls of narrow annuli need to be studied through corresponding visual experiments. On the other hand, for the fluid in narrow annuli is bilaterally heated, the fluid can get heat from the inside and outside walls and hereby the occurrence of ONB needs less heat compared with that in conventional channels. As shown in Fig. 7, the ONB heat flux calculated by Eq. (9), which is gotten from unilateral heating annular channel, is higher than the

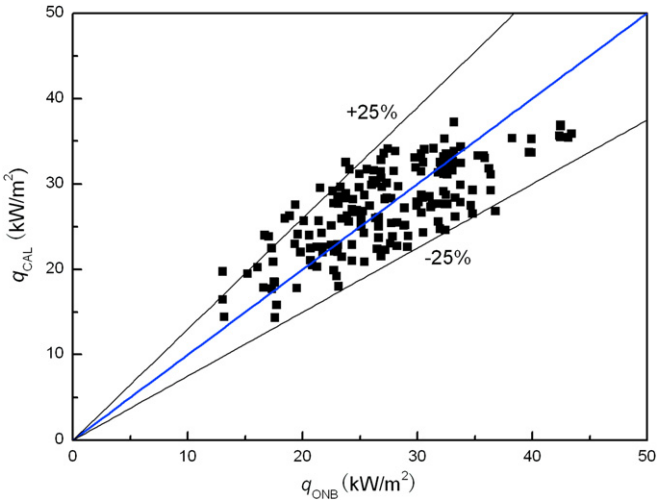

Fig. 8. Comparison between the experimental data and the results calculated by Eq. (13).

Table 3
List of part of experimental data.

s (mm)	Case	p (MPa)	G (kg/m^2 s)	Δt_{sat} (K)	q_o (kW/m^2)	q_{ONB} (kW/m^2)
(a) ONB occurring on inner annulus surface						
1.5	1	1.22	114.775	1.61	21.283	27.159
	2	1.44	111.71	2.44	25.808	33.18
	3	1.51	97.403	2.4	22.736	33.747
	4	1.64	111.1	1.89	20.659	32.267
	5	1.65	84.864	1.58	28.213	24.019
	6	1.71	70.502	1.76	28.69	25.244
	7	1.79	83.755	1.25	27.169	23.076
	8	1.85	56.146	1.48	31.454	25.322
	9	2.15	124.436	2.13	22.155	33.803
	10	3.08	138.687	1.46	21.149	26.323
	11	3.25	137.918	1.08	21.592	23.044
	12	3.76	79.226	0.88	15.751	20.861
2.0	1	2.2	105.733	2.79	32.385	38.241
	2	2.23	106.02	2.31	32.505	33.043
	3	2.3	86.194	2	26.01	23.768
	4	2.31	96.788	2.21	30.318	26.388
	5	2.32	96.453	2.6	29.836	29.793
	6	2.34	66.191	2.82	20.561	33.16
	7	2.35	85.828	2.01	27.937	23.368
	8	2.35	95.512	2.5	30.325	32.887
	9	2.38	97.153	1.95	30.593	23.03
	10	2.4	94.599	2.66	31.963	32.823
	11	2.42	93.321	2.39	32.226	32.785
	12	2.6	78.996	1.99	27.341	25.394
(b) ONB occurring on outer annulus surface						
0.95	1	1.03	128.76	1.34	19.896	27.722
	2	1.03	126.33	1.65	15.102	28.35
	3	1.04	115.03	2.03	21.253	32.588
	4	1.08	135.56	1.37	21.621	26.608
	5	1.08	142.2	1.65	21.626	29.945
	6	1.08	118.49	1.53	21.714	25.117
	7	1.08	134.79	1.76	21.774	30.351
	8	1.08	142.2	1.59	21.626	29.945
	9	1.1	115.47	1.12	26.981	20.691
	10	1.11	110.3	1.2	25.702	21.747
	11	1.11	125.03	1.39	33.1	21.253
	12	2.43	107.78	1.88	22.623	24.304
1.5	1	1.19	98.374	2.03	26.846	22.739
	2	1.28	103.145	1.79	27.309	23.859
	3	1.37	99.691	1.34	26.912	22.461
	4	1.4	103.346	2.06	32.779	25.832
	5	1.44	106.973	1.33	32.693	22.773
	6	1.56	68.948	1.7	15.207	24.394
	7	1.58	69.649	1.62	17.441	24.725
2.0	1	2.19	104.941	2.95	42.484	31.812
	2	2.23	106.02	3.11	33.043	32.505
	3	2.25	102.85	3.3	43.431	35.272
	4	2.32	96.453	2.8	29.793	29.836
	5	2.34	101.906	3.29	43.414	35.76
	6	2.35	95.512	2.8	32.887	30.325
	7	2.4	94.599	2.96	32.823	31.963
	8	2.44	79.031	2.24	18.549	26.847
	9	2.48	83.785	2.62	22.614	30.493
	10	2.49	85.755	2.91	23.086	31.414
	11	2.6	78.996	2.13	25.394	27.341
	12	2.79	85.04	2.21	39.933	31.166

experimental data. Thus this is the other reason of that the heat flux of ONB in the narrow annular channel is less than that in conventional channels or micro-tubes.

4.4. Experimental correlation for ONB in narrow annuli

The existed correlations are not applicable to narrow annuli and a new correlation for predicting the heat flux of the ONB in narrow annuli needs to be developed. As mentioned in Section 4.2, the factors affecting the heat flux of the ONB may be the mass flux G, the system pressure p, the wall superheat Δt_{sat}, the geometrical structure of the channel d_{oi}, d_{io} and the wall heat flux of the other side q [19,20]. Thus, the heat flux of the ONB is the following type of function:

$$q_{ONB} = f(G, p, \Delta t_{sat}, d_{oi}, d_{io}, q) \tag{10}$$

The following dimensionless parameters are introduced to develop the correlation with fully considering the above influencing factors. The influence of the mass flux G and the gap sizes on flow boiling heat transfer in narrow channels may be expressed by

the Reynolds number $\mathrm{Re} = Gs/\mu$ [11]. The density ratio ρ_g/ρ_f reflects the effect of the pressure and was hereby used to develop the correlation [21–23]. The dimensionless wall superheat is defined by $\Delta t^*_{sat} = \Delta t_{sat}/t_s$ and the channel geometry is reflected by the dimensionless diameter defined by $d^* = 2d_{j_1}/(d_{io} + d_{oi})$ where j_1 = io,oi. The dimensionless heat flux on the other side tube is given by $q^* = 2q/(q + q_{ONB})$ [20].

As discussed above, supposing that the heat flux of the ONB is in the derivation of power equation of the general form:

$$q_{ONB} = C\mathrm{Re}^a(\rho_g/\rho_f)^b \Delta t^{*c}_{sat} d^{*d} q^{*f} \tag{11}$$

Using linear regression, such equation is transformed by taking its logarithm to yield the following equation:

$$\log q_{ONB} = \log C + a\log \mathrm{Re} + b\log(\rho_g/\rho_f) + c\log \Delta t^*_{sat} + d\log d^* + f\log q^* \tag{12}$$

Thus, the results of the multi-variant linear regression analysis [24] are listed as following:

$$q_{ONB,m} = 241.048 \times \left(\frac{Gs}{\mu}\right)^{0.0256} \left(\frac{\rho_g}{\rho_f}\right)^{0.0562} \left(\frac{\Delta t_{sat}}{t_s}\right)^{0.448} \times \left(\frac{2d_{j_1}}{d_{io} + d_{oi}}\right)^{-0.134} \left(\frac{2q_n}{q_i + q_o}\right)^{-0.341} \tag{13}$$

where m = i, j_1 = io and n = o for the ONB occurring on the inside tube while m = o, j_1 = oi and n = i for the ONB occurring on the outside tube.

The relative error in Eq. (13) is defined by

$$\varepsilon = \frac{q_{EXP} - q_{CAL}}{q_{EXP}} \times 100\% \tag{14}$$

where q_{ExP} is the experimental heat flux and q_{CAL} is the heat flux obtained by Eq. (13). Fig. 8 shows the relative error of ±25% in Eq. (13). Part of experimental data is listed in Table 3.

5. Conclusions

Experimental study on CHF for the annular gap sizes of 0.95, 1.5 and 2.0 mm in cold-drawn SUS304 stainless steel narrow annuli with bilateral heating has been conducted. Through analyzing the experimental data, the main findings are as follows:

(1) The heat flux of the other side has great influence on the heat flux of the ONB and the heat flux of the ONB will decrease with the increase of the heat flux of the other side.
(2) The heat flux of the ONB in narrow annuli is much lower than that in conventional channels under the same conditions. The heat flux decreases as the gap size increases and there may be a critical size for the gap size where the heat flux of the ONB is the lowest under the same conditions.
(3) The correlation $q_{ONB} = 241.048 \times \mathrm{Re}^{0.0256}(\rho_g/\rho_f)^{0.0562}\Delta t^{*0.448}_{sat} d^* - 0.134 q^{*-0.341}$ may be used to estimate the heat flux of the ONB.

Acknowledgements

This work is financially supported by Program for New Century Excellent Talents in University (NCET-06-0837), to which the authors express their gratitude.

References

[1] Y. Sudo, M. Kaminaga, K. Minazoe, Experimental study on the effects of channel gap size on mixed convection heat transfer characteristics in vertical rectangular channels heated from both sides. Nucl. Eng. Des. 120 (2–3) (1990) 135–146.
[2] G.M. Mala, D.Q. Li, J.D. Dale, Heat transfer and fluid flow in microchannels. Int. J. Heat Mass Transfer 40 (13) (1997) 3079–3088.
[3] T.M. Adams, S.I. Abdel-Khalik, S.M. Jeter, Z.H. Qureshi, An experimental investigation of single-phase forced convection in microchannels. Int.J. Heat Mass Transfer 41 (6–7) (1998) 851–857.
[4] S.M. Ghiaasiaan, R.C. Chedester, Boiling incipience in microchannels. Int. J. Heat Mass Transfer 45 (23) (2002) 4599–4606.
[5] I. Hapke, H. Boye, J. Schmidt, Onset of nucleate boiling in minichannels. Int. J. Therm. Sci. 39 (4) (2000) 505–513.
[6] S.L. Qi, P. Zhang, R.Z. Wang, L.X. Xu, Flow boiling of liquid nitrogen in microtubes: part I - the onset of nucleate boiling, two-phase flow instability and two-phase flow pressure drop. Int. J. Heat Mass Transfer 50 (25–26) (2007) 4999–5016.
[7] J.R.S. Thom, W.M. Walker, T.A. Fallon, G.F.S. Reising, Boiling in subcooled water during flow up heated tubes or annuli, in: Symposium on Boiling Heat Transfer in Steam Generating Units and Heat Exchangers, Manchester, September. ImechE, London, 1965.
[8] W. Qu, I. Mudawar, Prediction and measurement of incipient boiling heat flux in micro-channel heat sinks. Int.J. Heat Mass Transfer 45 (19) (2002) 3933–3945.
[9] T. Chen, J.F. Klausner, S.V. Garimella, J.N. Chung, Subcooled boiling incipience on a highly smooth microheater. Int. J. Heat Mass Transfer 49 (23–24) (2006) 4399–4406.
[10] M. Kamil, M. Shamsuzzoha, S.S. Alam, Effect of submergence on boiling incipience in a vertical thermosiphon reboiler. Int. J. Therm. Sci. 44 (1) (2005) 75–87.
[11] S. Su, S. Huang, X. Wang, Study of boiling incipience and heat transfer enhancement in forced flow through narrow channels. Int. J. Multiphase Flow 31 (2) (2005) 253–260.
[12] S.J. Kline, F.A. McClintock, Describing uncertainties in single-sample experiments. Mech. Eng. 75 (1953) 3–12.
[13] R. Ahmadi, A. Nouri-Borujerdi, J. Jafari, I. Tabatabae, Experimental study of onset of subcooled annular flow boiling. Prog. Nucl. Energy 51 (2) (2009) 361–365.
[14] A.E. Bergles, W.M. Rohsenow, The determination of forced-convection surface-boiling heat transfer. J. Heat Transfer 86 (1964) 365–372.
[15] E.J. Davis, G.H. Anderson, The incipience of nucleate boiling in forced convection flow. AIChE J. 12 (4) (1966) 774–780.
[16] R. Hino, T. Ueda, Studies on heat transfer and flow characteristics in subcooled flow boiling—part 1. Boiling characteristics. Int. J. Multiphase Flow 11 (3) (1985) 269–281.
[17] C.L. Vandervort, A.E. Bergles, M.K. Jensen, Heat transfer mechanisms in very high heat flux subcooled boiling, in: Fundamentals of Subcooled Flow Boiling, HTD, vol. 217. ASME, 1992, pp. 1–9.
[18] J.E. Kennedy, G.M. Roach Jr., M.E. Dowling, S.I. AbdelKhalik, S.M. Ghiaasiaan, S. M. Jeter, Z.H. Qureshi, The onset of flow instability in uniformly heated horizontal microchannels. ASME J. Heat Transfer 122 (2000) 118–125.
[19] S.S. Bertsch, E.A. Groll, S.V. Garimell, Effects of heat flux, mass flux, vapor quality, and saturation temperature on flow boiling heat transfer in microchannels. Int. J. Multiphase Flow 35 (2) (2009) 142–154.
[20] Y.W. Wu, G.H. Su, S.Z. Qiu, B.X. Hu, Experimental study on critical heat flux in bilaterally heated narrow annuli. Int. J. Multiphase Flow 35 (11) (2009) 977–986.
[21] Y. Chang, S.C. Yao, Critical heat flux of narrow vertical annuli with closed bottoms. J. Heat Transfer 105 (1983) 192–195.
[22] S.H. Kim, W.P. Baek, S.H. Chang, Measurement of critical heat flux for narrow annuli submerged in saturated water. Nucl. Eng. Des. 199 (1–2) (2000) 41–48.
[23] S.Y. Chun, H.J. Chung, S.K. Moon, Critical heat flux under zero flow conditions in vertical annulus with uniformly and non-uniformly heated sections. Nucl. Eng. Des. 205 (3) (2001) 265–279.
[24] S.L. Xu, Common Algorithms Collection. Tsinghua University Press, 1995, pp. 372–376.